Dynamics of a Resistive Sheet Pinch

D. Biskamp
Max-Planck-Institut für Plasmaphysik Garching West Germany

Z. Naturforsch. **37 a**, 840–847 (1982); received April 6, 1982

To Professor Arnulf Schlüter on his 60th Birthday

The dynamic evolution and the saturated state of a long sheet pinch subject to growth of resistive tearing modes was investigated by numerical solution of the 2 D MHD equations. Both the compressible and the incompressible equations were used, and the difference is found to be negligible. The necessity of considering a resistive equilibrium is stressed. The paper concentrates on a static equilibrium maintained by an external electric field and requiring a special distribution of the resistivity η. In addition the dynamics of the resistivity plays an important part. Assuming η to be time independent, the sheet pinch develops a number of soliton-like magnetic islands, which coalesce. The final state consists of a single soliton, while the generation of further solitons is inhibited by a strong shear flow allong the current sheet. When allowance is made for parallel diffusion of the resistivity such that η is essentially a flux function, the final state is quite different. Here the longest wavelength dominates, leading to a single, large island and completely destroying the original sheet pinch.

I. Introduction

The tearing instability of a plane sheet pinch is the prototype of a resistive instability. It has been investigated in detail in the first paper on this topic by Furth, Killeen, and Rosenbuth (1963). Later the theory was generalized to more complex geometries, in particular cylindrical, to describe resistive modes in tokamaks. Nonlinear studies, primarily computations of the saturation widths of magnetic islands, have been performed in both plane and cylindrical geometry. While in the latter case island widths are computed quite accurately or estimated semiquantitatively by a simple criterion [1, 2], the attempts to calculate the saturation widths in the plane case seem to have been less successful. Although a number of papers treat the nonlinear evolution of tearing modes in a plane sheet pinch (see, for example, references 3 and 4), no generally accepted picture of the saturation width as a function of the wavelength or possibly other parameters has emerged.

The main difference seems to reside in two points: long wavelength and the question of resistive equilibrium. In the tokamak tearing mode computations unstable wave numbers are rather close to marginal conditions, at least for normal current profiles, and by choosing a resistivity profile inversely proportional to the current density one is dealing with a resistive equilibrium. The computed island widths are usually small, more or less independently of the time evolution of the resistivity, and there is quite good agreement with experimental observations [2]. On the other hand the sheet pinch configuration of most interest has spatial dimensions large compared with the thickness a of the current sheet and hence modes of long wavelength $k a \ll 1$, far from the marginal point $k a = 1$, have to be considered. However, no paper, treating the nonlinear behavior of tearing modes with $k a \ll 1$ is known to the author. In addition, a homogeneous resistivity distribution is usually assumed, probably for simplicity. Hence there is no resistive equilibrium, and the evolution of the modes is affected by the diffusive broadening of the current sheet. It should also be mentioned that little observational evidence of tearing modes in plane configurations exists.

We have therefore taken up this classical problem of 2 D tearing mode evolution in a plane sheet pinch, generalizing previous attempts and trying to avoid their shortcomings. We begin in Sect. II by briefly reviewing the linear stability theory, in particular the case of nonsymmetric position of the resonant surface, and also present some numerical results for finite values of the resistivity. In Sect. III we discuss the basic equations and indicate the numerical methods of solution. To solve a certain controversy that seems to have arisen in the recent literature, we study both the 2 D compressible MHD equations and the incompressible limit. In Sect. IV

Reprint requests to Dr. D. Biskamp, Max-Planck-Institut für Plasmaphysik, D-8046 Garching.

0340-4811 / 82 / 0800-0840 $ 01.30/0. — Please order a reprint rather than making your own copy.

we stress the necessity of a resistive equilibrium and discuss several types of equilibria that exist owing to different driving conditions. In addition to the question of equilibrium, the nonlinear behavior may strongly depend on the way the resistivity distribution evolves in time, particularly for large island size. We therefore consider the nonlinear development and saturation of tearing modes for two resistivity models. In Sect. V we treat the case of a static resistivity, while in Sect. VI we allow for the evolution of the resistivity distribution owing to convection and parallel diffusion. Section VII summarizes the results and presents some speculations on the general three-dimensional behavior.

II. Review of Linear Theory

Let us briefly recall the basic properties of the tearing instability. Throughout the paper we consider the equilibrium current density (in the z-direction) most frequently chosen:

$$j_0(x) = B_0/a \cosh^2(x/a). \tag{1}$$

The equilibrium magnetic field depends on the boundary conditions for large $|x|$. For the tearing mode to be unstable $\boldsymbol{B}$ or some component B_y of $\boldsymbol{B}$ must pass through zero at some surface x_s within the current sheet $|x_s| \lesssim a$,

$$B_y(x) = B_0 \left(\tanh \frac{x}{a} - \tanh \frac{x_s}{a} \right) = \psi_0' \tag{2}$$

with the magnetic flux

$$\psi_0(x) = B_0 a \left\{ \log \left(\cosh \frac{x}{a} \right) - \frac{x}{a} \tanh \frac{x_s}{a} \right\}. \tag{3}$$

We assume a magnetic pertubation $\boldsymbol{B}_1 = \hat{z} \times \nabla \psi_1$, $\psi_1 = \psi_1(x) \exp(i k_y y)$, giving rise to a plasma flow $\boldsymbol{v}_1 = \hat{z} \times \nabla \varphi_1$, $\varphi_1 = \varphi_1(x) \exp(i k_y y)$ which is conventionally assumed to be incompressible since the phase velocity of the mode is small compared with the sound speed. We shall see in Sect. III that the effect of plasma compressibility is also negligible in the nonlinear phase of the instability. The linearized MHD equations in this limit reduce to two equations for ψ_1 and φ_1:

$$\partial \psi_1 / \partial t - i k_y \psi_0' \varphi_1 = \eta (\psi_1'' - k_y^2 \psi_1), \tag{4}$$

$$\frac{\partial}{\partial t} (\varphi_1'' - k_y^2 \varphi_1) = i k_y \{ \psi_0' (\psi_1'' - k_y^2 \psi_1) - \psi_1 j_0' \}, \tag{5}$$

where we have introduced the following units: a, B_0, $v_A = B_0/\sqrt{(4\pi \varrho_0)}$, and ϱ_0. In these units η is the inverse magnetic Reynold's number S^{-1}, $S = 4\pi v_A a/\eta c^2$. The density $\varrho = \varrho_0$ is assumed to be homogeneous, while the pressure is eliminated by the assumption of incompressibility. With $\psi_1, \varphi_1 \propto \exp(\gamma t)$, (4) and (5) constitute an eigenvalue problem for the growthrate γ which has been solved by Furth, Killeen, and Rosenbluth [1] for sufficiently small η. The tearing mode is unstable for $k_y < 1$ (for $x_s = 0$ the threshold is exactly unity, while for $x_s \neq 0$, $x_s \lesssim 1$, it is slightly larger). For not too small k_y the constant-ψ approximation is valid. Here an analytical expression is given:

$$\gamma \cong 0.5 (k_y \psi_0'')^{2/5} \eta^{3/5} \Delta'^{4/5}, \tag{6}$$

where $\Delta = (\psi_{1-}' - \psi_{1+}')/\psi_1$. For $k_y \ll 1$ it is found that

$$\Delta' = \frac{\psi_0''(x_s)^2}{k_y} \left[\frac{1}{\psi_0'(+\infty)^2} + \frac{1}{\psi_0'(-\infty)^2} \right] = 2 \cosh(2 x_s)/k_y \cosh^2 x_s \tag{7}$$

which does not vary very strongly with x_s. It thus follows that

$$\gamma \cong \eta(x_s)^{3/5} k_y^{-2/5} \cosh^{-4/5}(x_s). \tag{8}$$

It appears that because of the last factor the symmetric case $x_s = 0$ is the most unstable. However, the x_s dependence of the first factor should not be overlooked. Let us consider a current sheet with a strong constant component of $\boldsymbol{B}$, B_z, parallel to the current direction, and admit tearing modes of general wave vector $\boldsymbol{k} = (k_y, k_z)$, the possible values of k_z being determined by the boundary conditions in the z direction. The position of the resonant surface is determined by $k_y B_y(x) + k_z B_z = 0$. All these different modes may grow simultaneously and their relative growthrates depend on the resistivity profile. If we assume a static resistive equilibrium, which implies $\eta(x) \propto j_0^{-1}(x) = \cosh^2 x$, we find $\gamma \propto \cosh^{2/5} x_s$. Hence modes with $x_s \neq 0$ would grow faster than the central modes. On the other hand, the growthrate is not a good indicator of the mode's actual importance. As we shall see in Sect. V, the saturation island size is smaller for $x_s \neq 0$ despite the larger growthrates.

Equations (6) and (8) indicate that because of $\Delta' \propto k_y^{-1}$ the growthrate increases with decreasing k_y down to a value k_m, where the constant-ψ approximation becomes invalid. An estimate of k_m can be obtained in the following way. The constant-ψ

approximation breaks down if Δ' approaches δ^{-1}. δ = resistive layer width, where the variation of ψ within δ, $\Delta\psi/\psi$, becomes of order unity. Within the resistive layer the diffusion term dominates in eq. [4]. With $\psi_1'' = \psi_1 \Delta'/\delta$ we have $\gamma\psi_1 \cong \eta\Delta'\psi_1/\delta$ and hence $\delta \cong \eta\Delta'/\gamma$. For $\Delta' \cong \delta^{-1}$ this implies that $\gamma/\eta \cong \Delta'^2$, and hence the wave number k_m, where the growthrate is largest, is of the order

$$k_m \cong \eta^{1/4} f(x_s), \quad f = 0(1) \tag{9}$$

and the maximum growthrate is

$$\gamma_m \cong \eta^{1/2} g(x_s), \quad g = 0(1). \tag{10}$$

For $k \lesssim k_m$, where the eigenvalue equations have been treated numerically in Ref. [5], γ decreases monotonically to zero at $k = 0$.

These results are derived by making use of the smallness of the resistivity. To obtain an idea of how small η must be for the results to be valid, we integrated (4) and (5) numerically in time for a number of intermediate η values. Figure 1 presents the growth rates $\gamma(k)$ for boundary conditions corresponding to a conducting wall at $L_x = 10$ as well as $L_x = \infty$, making use of the asymptotic behavior $\psi_1 \propto \exp\{-k_y|x|\}$. The presence of a wall has a noticeably stabilizing effect only on modes with $k_y < 2L_x^{-1}$. Apart from the regime of very small k_y

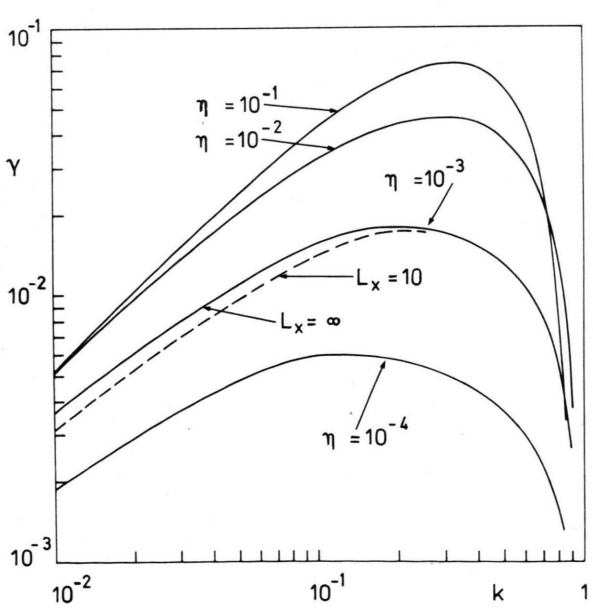

Fig. 1. Linear growth rate $\gamma(k)$ for different values of η. Solid lines for open system $L_x = \infty$, dashed line for conducting wall at $x = \pm L_x$, $L_x = 10$.

the analytical results predict the actual γ values quite accurately for $\eta \lesssim 10^{-2}$, and also for $\eta = 10^{-1}$ the prediction is still qualitatively correct. In the nonlinear computations discussed in the remaining sections we restrict ourselves to $10^{-2} \geqq \eta \geqq 10^{-3}$, $20 \geqq L_x \geqq 10$ and modes with $0.5 \gtrsim k_y \gtrsim 0.1$.

III. Basic Equations and Numerical Procedures

We consider two different two-dimensional MHD models, 1) a compressible MHD system with vanishing normal magnetic field B_z, and 2) the incompressible limit of 1), which can also be considered as the opposite limit of a strong normal field $B_z \gg B_x, B_y$ giving rise to incompressible $\boldsymbol{E}\times\boldsymbol{B}$ motions in the (x, y) plane. The equations of system 1) are

$$\varrho\left(\frac{\partial \boldsymbol{v}}{\partial t} + \boldsymbol{v}\cdot\nabla\boldsymbol{v}\right) = -\nabla p - \nabla\psi\, j_z, \tag{11}$$

$$\frac{\partial\psi}{\partial t} + \boldsymbol{v}\cdot\nabla\psi = \eta\, j_z - E_0, \tag{12}$$

$$\frac{\partial\varrho}{\partial t} + \boldsymbol{v}\cdot\nabla\varrho = -\varrho\,\nabla\cdot\boldsymbol{v}, \tag{13}$$

$$\frac{\partial p}{\partial t} + \boldsymbol{v}\cdot\nabla p = -2p\,\nabla\cdot\boldsymbol{v}, \tag{14}$$

where $\boldsymbol{B} = (B_x, B_y) = \hat{z}\times\nabla\psi$, $\boldsymbol{j} = (0, 0, \nabla^2\psi)$, $\boldsymbol{v} = (v_x, v_y)$. E_0 is an integration constant which can be interpreted as the electric field applied to the system at the boundary, and which with an appropriate resistivity distribution allows for a static resistive equilibrium. Equations (11) – (14) are solved in a rectangular system $-L_x \leqq x \leqq L_x$, $0 \leqq y \leqq L_y$ with a rigid conducting wall at $\pm L_x$ implying $v_x(\pm L_x) = 0$ and the magnetic flux enxlosed in the system $\psi(L_x) - \psi(-L_x)$ fixed in time, and imposing periodic boundary conditions in the y direction. The equilibrium current distribution and magnetic field are given by eqs. (1) and (2), while the pressure results from the balance $p_0(x) + B_y^2(x)/2 = P_0 =$ const. The finite difference scheme is a variant of spatial resolution in the vicinity of the resonant the FCT methods [6]. To provide for adequate surface a non-equidistant mesh is used in the x direction. Typically $\Delta x_{\min} \leqq 0.1$ at $x \cong x_s$, while $\Delta x_{\max} \cong 1$ for $|x| \gg 1$.

The second system investigated is the incompressible limit of eqs. (11) – (14), which results either from choosing a high background pressure $P_0 \gg 1$

(high β limit) or, as mentioned before, by assuming a large, normal magnetic field B_z (low β limit). For simplicity we choose a homogeneous density $\varrho = 1$. Taking the curl of eq. (11) eliminates the pressure as an independent dynamic variable and yields an equation for the vorticity function W

$$\partial W/\partial t + \boldsymbol{v}\cdot\nabla W = \hat{z}\cdot(\nabla\psi \times \nabla\nabla^2\psi) \tag{15}$$

which is related to the stream function φ by $W = \nabla^2\varphi$ with $\boldsymbol{v} = \hat{z}\times\nabla\varphi$. Equation (12) for ψ remains unchanged. Hence there are only two quantities to be computed, φ and ψ, instead of five in the compressible system. More importantly from the computational point of view is the fact that the fast compressional wave is eliminated, which allows substantially larger time steps and hence computational economy. As in the compressible case we use a Cartesian mesh in x and y with grid point concentration around x_s and with equivalent boundary conditions. Poisson's equation is solved by a hybrid scheme using fast Fourier transform in y and tridiagonal matrix inversion in x to allow for the non-equidistant grid point spacing.

For all problems considered the difference between both models has been found to be practically negligible. Because of the relatively slow phase and plasma velocities involved even in the fast resistive processes such as island coalescence the plasma motion is to a high degree incompressible. Most of the computation reported in the subsequent sections of this paper were therefore performed using the incompressible model.

IV. Resistive Equilibrium

The linear tearing instability only depends on the value of the resistivity (or the resistivity gradient in the case of the rippling mode not considered here) at the resonant surface x_s. Since the growth rate, which scales as a fractional power of the resistivity, is large compared with the rate of global current diffusion, the latter is neglected in linear theory. At finite amplitude or magnetic island size, however, the dynamic evolution takes place on the diffusion time scale, as was first pointed out by Rutherford [7], and is therefore expected to be influenced by the evolution of the average current profile. If a homogeneous resistivity $\eta = \eta_0$ is assumed, as is frequently done, the current sheet system is evidently not in resistive equilibrium but broadens diffusively on the resistive time scale. When perturbing this system by a tearing mode of small amplitude we find that after an initial phase of growth the mode decays. The maximum amplitude reached during this process strongly depends on both η_0 and the initial amplitude, and the maximum island width is in general small compared with the width of the current sheet. A current sheet can thus only be significantly affected by the tearing instability if it is maintained for a sufficiently long time, i. e. if there is some kind of resistive equilibrium. We may distinguish between essentially two types of resistive equilibria. On the one hand, the current layer is maintained by counterstreaming plasma flows. The prototype is the Sweet-Parker model of magnetic reconnection. In this case there is, however, an inhomogeneous plasma flow along the magnetic field in the current layer, which would not be compatible with the periodic boundary conditions assumed in this paper. Tearing mode growth of this kind has recently been investigated in the current layer between two coalescing magnetic islands [8]. In the absence of plasma flows an equilibrium state requires an externally applied electric field E_0. Current density and resistivity adjust themselves in such a way that $\eta j_0 = \text{const}$ as seen from (12). These are roughly the conditions in the quasi-steady state of a tokamak discharge. In the present paper we shall restrict ourselves to the case of static resistive equilibrium.

Since the resistivity profile is inhomogeneous, it will in general evolve in time. In the nonlinear theory of tearing modes in tokamak-like plasmas it is often assumed for simplicity that the resistivity profile remains fixed, $\eta = \eta_0(r)$. This is certainly not correct since because of the high parallel thermal condition of the electrons $\eta = \eta(T_e)$ is to a large extent a flux function, $\eta = \eta(\psi)$. Numerical computations, however, taking the time variation of η into account reveal that the difference is rather insignificant, which justifies the simplifying assumption of a static η profile. As discussed in the introduction, tearing modes in tokamaks correspond to $k \sim 1$, while in the present paper we are mainly interested in long-wavelength modes $k \ll 1$. We therefore investigate both cases of a static resistivity, Sect. V, and a dynamically evolving resistivity profile,

$$\frac{\partial\eta}{\partial t} + \boldsymbol{v}\cdot\nabla\eta = \varkappa_{\parallel}\nabla_{\parallel}^2\eta \tag{16}$$

in Section VI. As we shall see, the latter model entails basically different saturation properties of tearing modes. The resistivity model (16) has been chosen for simplicity. It is somewhat different from assuming a collisional resistivity $\eta(T) \propto T^{-3/2}$ where T satisfies Eq. (16), but we expect the difference to be qualitatively unimportant.

V. Saturation of Tearing Mode for a Static Resistivity Model

In this section we choose a time-independent resistivity model in eq. (12), $\eta = \eta(x) = \eta_0/j_0(x)$, and the applied electric field $E_0 = \eta_0$. As a consequence of this choice the saturated island state cannot be a static configuration, but requires a plasma flow $\boldsymbol{v}$, $\boldsymbol{v} \cdot \nabla \psi = \eta_0 (j_f - j_0)$ where $j_f = j_f(\psi)$ is the final current distribution. We investigated the size of the saturated islands varying the wave number k of the initial perturbation as well as η_0. We also considered the asymmetric case $x_s \neq 0$. The distance of the confining walls $\pm L_x$ was chosen $L_x = 10$ such that the size of islands is independent of L_x. The main results are:

a) The island size W_I increases with decreasing k in the regime which corresponds approximately to the right-hand part of the dispersion curve $1 > k > k_m$, where k_m is given by eq. (9). The islands of different wavelengths are self-similar, width and length being proportional.

b) No islands of wave number $k < k_m$ are formed. In a sheet pinch of large dimensions, $L_y \gg k_m^{-1}$, several islands of wave number $k \cong k_m$ are formed. These tend to coalesce. The result of coalescence o af pair of k_m islands is again a k_m island. These isolated islands may be called magnetic solitons. The final state is a single soliton moving with a certain velocity v_0 either to the right or to the left, depending on the initial conditions. The magnitude of v_0 does not seem to depend on the system length L_y but only on the resistivity. We find $v_0 \propto \eta^{1/2}$ approximately. The neutral sheet between these final solitons is stable with respect to tearing modes owing to a strong shear flow along the sheet, the magnitude of which increases with increasing L_y and is much larger than the soliton velocity v_0.

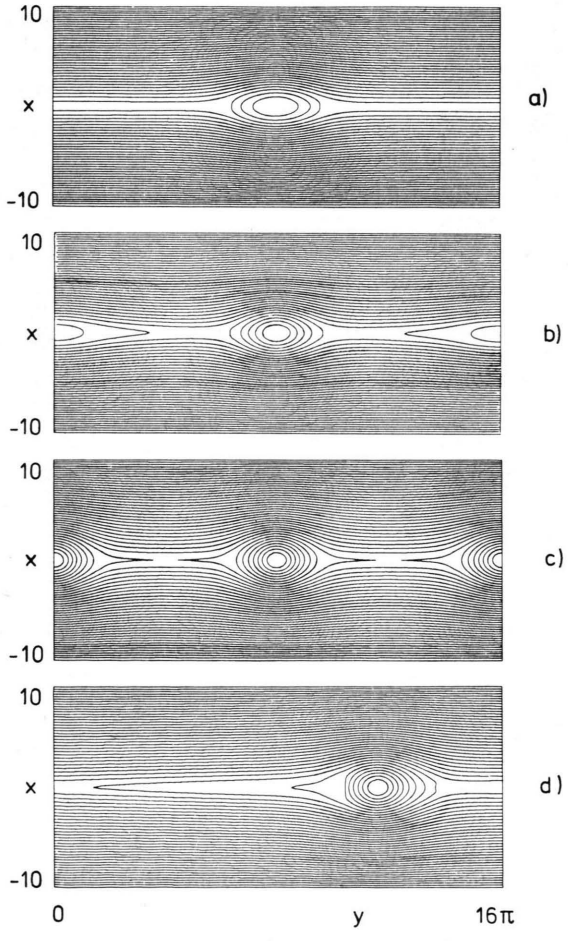

Fig. 2. Time evolution of islands for a static resistivity profile $\eta(x) = 10^{-2}/j_0(x)$. Contours of $\psi(x,y)$ at a) time $t = 200$; b) $t = 400$; c) $t = 1000$; d) $t = 8000$.

Figure 2 shows the development of islands with a periodicity length $L_y = 16\pi$ and $\eta_0 = 10^{-2}$. Only the smallest wave number $k = 0.125$ was excited at time $t = 0$. It soon gives rise to formation of a single soliton of spatial dimensions corresponding to a dominant wave number $k \cong k_m \cong 0.3$. The current layer between two solitons, however, becomes unstable and a further k_m soliton is generated. Owing to the symmetry of the formation process a long time passes until a coalescence instability develops at $t \sim 4000$ from round-off errors. The final result is again a single soliton which, however, is now not at rest but moves with constant speed $v_0 = 0.056$ to the left. Note this asymmetry which has developed spontaneously due to the asymmetry of round-off errors. With more general and less symmetric initial conditions this final state is reached much sooner. In Fig. 3 we see the final state for $\eta_0 = 3 \times 10^{-3}$. Here the soliton moves to the right, $v_0 =$

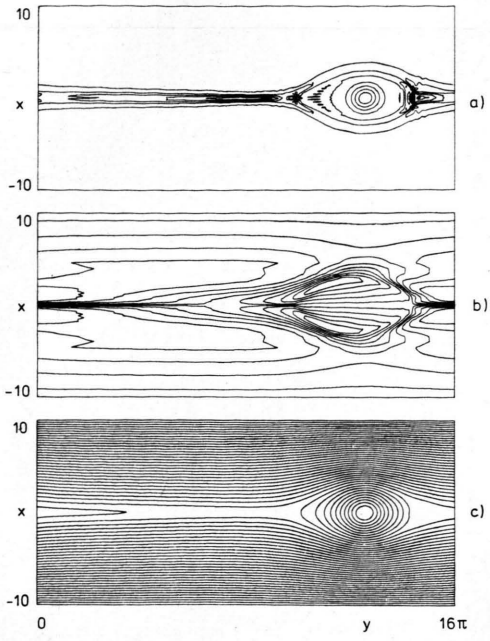

Fig. 3. Final state $t=8000$ as in Fig. 2d, but with $\eta(x)=3\times10^{-3}/j_0(x)$. a) $j(x,y)$; b) $\varphi(x,y)$; c) $\psi(x,y)$.

-0.027. It should be noted that the asymmetry is not in conflict with momentum conservation which is automatically satisfied by the boundary condition $\varphi(\pm L_x)=0$.

In the asymmetric case, $x_s\neq0$, saturation amplitudes rapidly decrease with increasing $|x_s|$ (see Fig. 4) although the linear growth rates are larger,

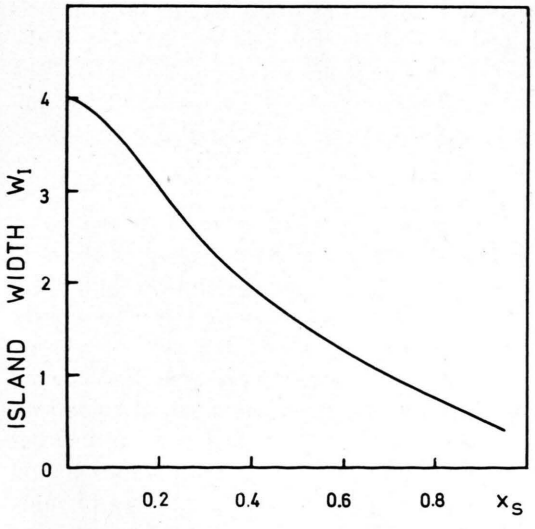

Fig. 4. Saturation island width W_I for static resistivity $\eta(x)$ as a function of the position x_s of the resonant layer.

as discussed in Section II. The dependence on the wavelength is qualitatively the same as for $x_s=0$, in particular there being no long-wavelength islands.

The absence of magnetic islands or solitons of longer wavelength and larger size is apparently due to the fixed resistivity distribution. Consider the ψ – equation (12) averaged over y

$$\frac{\partial\psi_0(x,t)}{\partial t}+\langle\boldsymbol{v}\cdot\nabla\psi\rangle_y=\eta(x)\,(j_0(x,t)-j_0(x,0))\,. \tag{17}$$

A large size island would generate an average current distribution $j_0(x,t)$ strongly deviating from the equilibrium current $j_0(x,0)$. So the r.h.s. of (17) $\eta(x)\delta j_0(x)$ tends to restore the original current distribution. Another way of arguing is to point out the flows associated with the variation of the resistivity along the flux surfaces. Noting that $\langle\boldsymbol{v}\cdot\nabla\psi\rangle_\psi$ averaged over a flux surfaces vanishes, equation (12) can be written in the stationary case in the form

$$\boldsymbol{v}\cdot\nabla\psi=(\eta-\langle\eta\rangle_\psi)\,j(\psi)\,. \tag{18}$$

Hence the plasma flow velocity increases with increasing island size. Since the resistivity is large outside the current sheet, the kinetic energy associated with the plasma flow becomes a significant fraction of the available free magnetic energy if the island size exceeds the current sheet thickness, which effectively limits the final island size.

Let us briefly comment on a recent article by Hayashi [4], where the author claims that the spontaneous process of island coalescence investigated by Pritchett and Wu [9] and by Biskamp and Welter [10] does not take place for islands generated by the resistive tearing instability. This is attributed to the numerically observed current distribution with j being larger at the x-points than at the 0-points, which counteracts the mutal attraction of the islands. Apparently, the islands generated in Hayashi's computations are rather small because of the assumption of a homogeneous η distribution (see our discussion in Section IV). We, too, find this behaviour of the current density, but it becomes less pronounced as the island width increases. Spontaneous island coalescence takes place even if in a small region around the x-point j is larger than within the island, because this process depends on the global current distribution.

VI. Effects of Dynamic Resistivity Behavior

The static resistivity model of the previous section represents a rather artificial assumption which is difficult to justify on physical grounds. This is especially true if large islands occur where η would vary appreciably across the island. We therefore investigated a more realistic behaviour of η, eq. (16), taking into account both convection with the plasma velocity $\boldsymbol{v}$ and diffusion along the magnetic field, where the latter process is in often the dominant one, making η essentially a flux function $\eta(\psi)$. Perpendicular diffusion $\varkappa_\perp$ as well as ohmic heating or other energy sinks or sources will usually only play a role on the longer transport time scale, where the manner of sustaining the equilibrium would also matter.

For short periodicity length L_y allowing only for modes with $k \gtrsim 0.5$ the behavior is quite similar to the case with static resistivity, the saturated islands being somewhat larger. For larger L_y only the first phase of the island evolution resembles the static η case. Because of the increase of the resistivity due to both plasma flow and η diffusion along the separatrix the current density in the x-point region becomes smaller and is more and more concentrated in the island interior, while the island continues to grow to a large final size. If several islands are created initially they will coalesce in an early stage of the evolution. Hence the final state of the tearing instability in a sheet pinch of periodicity length L_y is a single island, as shown in Figure 5. (A similar behavior has recently been found for the collisionless tearing mode [11].) The islands are self-similar, width and wavelength being proportional. The final state is a new essentially static equilibrium with $\eta(\psi) j(\psi) = E_0$. For large L_y (and L_x) this configuration tends toward the one generated by a periodic sequence of line currents flowing at the 0-points. In this case the flux function is given by

$$\psi = \frac{L_y}{2\pi} \ln \left(\cosh \frac{2\pi x}{L_y} + \cos \frac{2\pi y}{L_y} \right) \qquad (19)$$

leading to an island width $W_I = 0.56\, L_y$. For the islands shown in Fig. 5 we find $W_I \cong 0.4\, L_y$. This is, however, not due to L_y (or L_x) being too small for the asymptotic formula (19) to be valid but to the fact that the original resistivity distribution was chosen $\eta(x) = \eta_0 \cosh^2 x/(1 + 0.03 \cosh^2 x)$ allowing for a finite value $\eta = 33\, \eta_0$ for $|x| \to \infty$. After island formation η and hence j are finite outside the main current carrying region at the 0-point, $j = 0.03$. Though this is small compared to the maximum value $j = 1$ at the 0-point, it is sufficient to reduce the island width to the value observed. In particular the angle of the separatrix at the x-point is smaller than 90°, which value would be expected if j vanishes.

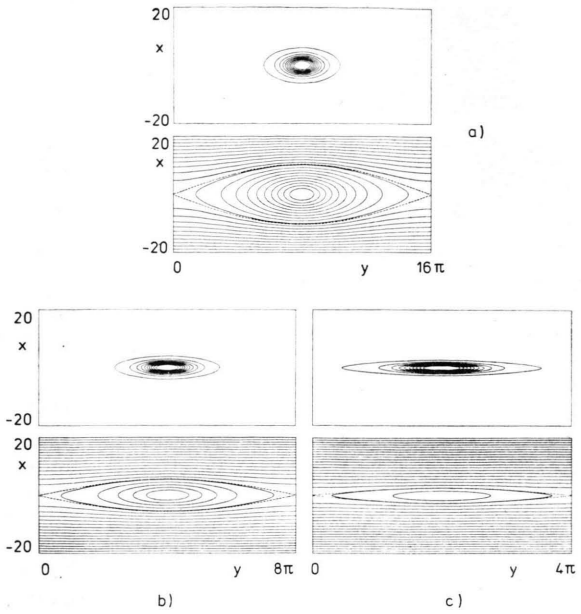

Fig. 5. Final distributions of $j(x,y)$ and $\psi(x,y)$ for a dynamically evolving resistivity for different system lengths a) $L_y = 16\pi$; b) $L_y = 8\pi$; c) $L_y = 4\pi$.

The final island size is practically independent of the magnitude of the resistivity η_0, as long as it is small, and also of the value of $\varkappa_\parallel$, at least if the diffusion term dominates in Equation (16). The case, where this term is small compared to the convection term, has not been considered.

VII. Conclusions

In this paper we have given a picture of the two-dimensional, dynamic evolution of a long sheet pinch configuration due to finite resistivity. To clarify some recent arguments about the role of plasma compressibility, both the compressible and the incompressible MHD equations were solved numerically. In all cases considered the difference turned out to be negligible, in agreement with intuition and with a recent investigation of the process of magnetic island coalescence [8]. It is well-known that the nonlinear evolution of tearing modes is a slow,

resistive diffusion process on the same time scale as the resistive broadening of the current sheet. We have shown that in general the latter effect has a strongly stabilizing influence. The physically more relevant question is the stability of a current sheet maintained from outside for a period long compared with the resistive decay time, i. e. which is in some kind of resistive equilibrium. While we we previously [8] studied the effect of tearing modes in a current layer maintained by counter streaming plasma flows, we now concentrate on the case of a static equilibrium driven by an external electric field and requiring a resistivity distribution $\eta \propto j^{-1}$.

Whereas for typical tokamak current profiles only tearing modes with wave numbers of the order of the marginal wave number exist for topological reasons ($k \sim m \sim 1$), the emphasis in the present paper is on long-wavelength modes ($k \ll 1$). Since these may lead to islands of large size $W_I \gtrsim 1$, the dynamic behavior of the resistivity is expected to play an important role. We have therefore investigated two different resistivity models. a) For the somewhat artificial case of a static resistivity profile the main result is that a long current sheet breaks up into a number of soliton-like magnetic islands with $k \sim k_m \sim \eta^{1/4}$ and island size $W_I \propto k_m^{-1}$, which tend to coalesce. The final state consists of a single k_m soliton, moving at a certain speed v_0 depending only on the magnitude of the resistivity. The current layer is stable against generation of further solitons due to a strong shear flow. b) In the more realistic case of high parallel resistivity diffusion (heat conduction) the final state is quite different. Here only one large island remains with $k L_y \cong 1$, where L_y is the length of the system. The current sheet is completely destroyed, the final distribution being an isolated pinch of about circular shape. What happens in an actual physical situation is largely determined by the boundary conditions, such as the presence of walls, externally forced plasma flows and energy sources and sinks to control the resistivity distribution.

Finally, we should like to underline that the present results are restricted to two-dimensional geometry. The completely coherent behavior, i. e. absence of small-scale turbulence, observed in all computations is certainly due to this geometric restriction. Admitting variations in the third direction allows simultaneous growth and interaction of modes with different orientations of wave vectors (different "helicities"), which is known from tokamak theory to give rise to intense small-scale turbulence [12]. The three-dimensional behavior of a sheet pinch is currently under investigation.

Acknowledgement

The author would like to thank Mrs. M. Walter for carrying out the programming for the numerical computations.

[1] R. B. White, D. A. Monticello, M. N. Rosenbluth, and B. V. Waddell, Phys. Fluids **20**, 800 (1977).
[2] J. D. Callen, B. V. Waddell, B. Carreras, M. Azumi, P. J. Catto, H. R. Hicks, J. A. Holmes, D. K. Lee, S. J. Lynch, J. Smith, M. Soler, K. T. Tsang, and J. C. Whitson, Plasma Physics and Controlled Nuclear Fusion Research 1978, IAEA, Vienna 1979, Vol. I, p. 415.
[3] W. H. Matthaeus and D. Montgomery, J. Plasma Phys. **25**, 11 (1981).
[4] T. Hayashi, J. Phys. Soc. Japan **50**, 3124 (1981).
[5] H. P. Furth, J. Killeen, and M. N. Rosenbluth, Phys. Fluids **6**, 459 (1963).
[6] D. L. Book, J. P. Boris, and K. Hain, J. Comp. Phys. **18**, 248 (1975).
[7] P. H. Rutherford, Phys. Fluids **16**, 1903 (1973).
[8] D. Biskamp, Phys. Lett. **87A**, 357 (1982).
[9] P. L. Pritchett and C. C. Wu, Phys. Fluids **22**, 2140 (1979).
[10] D. Biskamp and H. Welter, Phys. Rev. Lett. **44**, 1069 (1980).
[11] I. Katanuma, and T. Kamimura,, Phys. Fluids **23**, 2500 (1980).
[12] B. V. Waddell, B. Carreras, H. R. Hicks, and J. A. Holmes, Phys. Fluids **22**, 896 (1979).